Title
Tumor Sink Effect in 68Ga-PSMA-11 PET: Myth or Reality?

Journal
Journal of Nuclear Medicine, 63(2)

ISSN
0161-5505

Authors
Gafita, Andrei
Wang, Hui
Robertson, Andrew
et al.

Publication Date
2022-02-01

DOI
10.2967/jnumed.121.261906

Peer reviewed

Tumor Sink Effect in ^{68}Ga-PSMA-11 PET: Myth or Reality?

Andrei Gafita[1,2]*, Hui Wang[2]*, Andrew Robertson[2], Wesley R. Armstrong[1], Raphael Zaum[2], Manuel Weber[3], Farid Yagubbayli[2], Clemens Kratochwil[4], Tristan R. Grogan[5], Kathleen Nguyen[1], Fernando Navarro[2,6], Rouzbeh Esfandiari[7], Isabel Rauscher[2], Bjoern Menze[6,8], David Elashoff[5], Ebrahim S. Delpassand[7], Ken Herrmann[3], Johannes Czernin[1], Michael S. Hofman[9], Jeremie Calais[1], Wolfgang P. Fendler[3], and Matthias Eiber[2]

[1]*Ahmanson Translational Theranostics Division, Department of Molecular and Medical Pharmacology, UCLA, Los Angeles, California;* [2]*Department of Nuclear Medicine, Klinikum rechts der Isar, Technical University Munich, Munich, Germany;* [3]*Department of Nuclear Medicine, University of Duisburg–Essen and German Cancer Consortium–University Hospital Essen, Essen, Germany;* [4]*Department of Nuclear Medicine, Heidelberg University Hospital, Heidelberg, Germany;* [5]*Department of Medicine Statistics Core, David Geffen School of Medicine, UCLA, Los Angeles, California;* [6]*Department of Informatics, Technical University Munich, Munich, Germany;* [7]*Excel Diagnostics and Nuclear Oncology Center, Houston, Texas;* [8]*Department of Quantitative Biomedicine, University of Zurich, Zurich, Switzerland; and* [9]*Prostate Cancer Theranostics and Imaging Centre of Excellence, Molecular Imaging and Therapeutic Nuclear Medicine, Peter MacCallum Cancer Centre, and Sir Peter MacCallum Department of Oncology, University of Melbourne, Melbourne, Victoria, Australia*

We aimed to systematically determine the impact of tumor burden on ^{68}Ga-prostate-specific membrane antigen-11 (^{68}Ga-PSMA) PET biodistribution by the use of quantitative measurements. **Methods:** This international multicenter, retrospective analysis included 406 men with prostate cancer who underwent ^{68}Ga-PSMA PET/CT. Of these, 356 had positive findings and were stratified by quintiles into a very low (quintile 1, $\leq$25 cm^3), low (quintile 2, 25–189 cm^3), moderate (quintile 3, 189–532 cm^3), high (quintile 4, 532–1,355 cm^3), or very high (quintile 5, $\geq$1,355 cm^3) total PSMA-positive tumor volume (PSMA-VOL). PSMA-VOL was obtained by semiautomatic segmentation of total tumor lesions using qPSMA software. Fifty prostate cancer patients with no PSMA-positive lesions (negative scan) served as a control group. Normal organs, which included salivary glands, liver, spleen, and kidneys, were semiautomatically segmented using ^{68}Ga-PSMA PET images, and SUV_{mean} was obtained. Correlations between the SUV_{mean} of normal organs and PSMA-VOL as continuous and categoric variables by quintiles were evaluated. **Results:** The median PSMA-VOL was 302 cm^3 (interquartile range [IQR], 47–1,076 cm^3). The median SUV_{mean} of salivary glands, kidneys, liver, and spleen was 10.0 (IQR, 7.7–11.8), 26.0 (IQR, 20.0–33.4), 3.7 (IQR, 3.0–4.7), and 5.3 (IQR, 4.0–7.2), respectively. PSMA-VOL showed a moderate negative correlation with the SUV_{mean} of the salivary glands ($r = -0.44$, $P < 0.001$), kidneys ($r = -0.34$, $P < 0.001$), and liver ($r = -0.30$, $P < 0.001$) and a weak negative correlation with the spleen SUV_{mean} ($r = -0.16$, $P = 0.002$). Patients with a very high PSMA-VOL (quintile 5, $\geq$1,355 cm^3) had a significantly lower PSMA uptake in the salivary glands, kidneys, liver, and spleen than did the control group, with an average difference of −38.1%, −40.0%, −43.2%, and −34.9%, respectively ($P < 0.001$). **Conclusion:** Tumor sequestration affects ^{68}Ga-PSMA biodistribution in normal organs. Patients with a very high tumor load showed a significantly lower uptake of ^{68}Ga-PSMA in normal organs, confirming a tumor sink effect. As similar effects might occur with PSMA-targeted radioligand therapy, these patients might benefit from increased therapeutic activity without exceeding the radiation dose limit for organs at risk.

Key Words: PET; tumor sink effect; prostate cancer; PSMA; Ga-PSMA; radioligand therapy

J Nucl Med 2022; 63:226–232
DOI: 10.2967/jnumed.121.261906

The biodistribution of radiolabeled prostate-specific membrane antigen (PSMA) ligands in prostate cancer patients reflects a complex interaction between tracer uptake, retention, and excretion in pathologic and normal tissues. Accumulation of PSMA ligands is also observed in nontumoral tissues, such as liver, spleen, kidneys and salivary glands, which have been shown to exhibit a high variability in tracer uptake (*1*). In clinical practice, it is observed that the relative accumulation of PSMA ligands in normal tissue is inversely related to the PSMA-positive tumor burden. This phenomenon is commonly referred to as the tumor sink effect, in which high tracer uptake in extensive tumor masses reduces tracer accumulation in normal tissues (*2–4*).

PSMA-targeted radioligand therapy with ^{177}Lu (^{177}Lu-PSMA-RLT) demonstrated positive results in phase II trials of men with metastatic castration-resistant prostate cancer (*5–7*) and is currently being investigated in the metastatic hormone-sensitive prostate cancer setting (*8*). If confirmed, a tumor sink effect might have implications for ^{177}Lu-PSMA-RLT by providing the rationale for individual adaptation of therapeutic dosages to the patient tumor load (*9*). Patients with a high tumor load might benefit from a higher injected activity per cycle without exceeding radiation dose limit in organs at risk, particularly the salivary glands and the kidneys, which are considered dose-limiting organs (*10*).

Besides their therapeutic use, PSMA ligands have also been applied for diagnostic purposes using tumor-specific whole-body PET imaging (e.g., ^{68}Ga-PSMA-11 [^{68}Ga-PSMA]) (*11*). ^{68}Ga-PSMA PET imaging provides reliable estimates of the biodistribution of therapeutic PSMA ligands (*12*). Several reports have previously investigated the sink effect in PSMA-targeted PET; however, the data reported are contradictory (*13*,*14*).

Received Jan. 4, 2021; revision accepted May 4, 2021.
For correspondence or reprints, contact Andrei Gafita (agafita@mednet.ucla.edu).
*Contributed equally to this work.
Guest editor: Todd Peterson, Vanderbilt University
Published online May 28, 2021.

To address this question, we aimed here to quantify the effect of tumor burden on ^{68}Ga-PSMA PET organ biodistribution by the use of quantitative measurements. We hypothesized that the tumor sequestration of the injected radiopharmaceutical in patients with a high disease burden leads to a significant decrease in uptake in nontumoral tissue.

MATERIALS AND METHODS

Study Design and Patient Population

Data of men with histologically proven prostate cancer who underwent ^{68}Ga-PSMA PET imaging at 6 institutions were screened retrospectively. This international multicenter study was designed to include patients with both PSMA-positive and PSMA-negative PET scans. First, 2 preestablished databases of patients with known metastatic disease on ^{68}Ga-PSMA PET were screened: the first was a dataset of men with metastatic hormone-sensitive prostate cancer who received ^{68}Ga-PSMA PET in the setting of initial staging or biochemical recurrence ($n = 100$), and the second was a dataset of men with metastatic castration-resistant prostate cancer who received ^{68}Ga-PSMA PET before initiation of ^{177}Lu-PSMA-RLT (*15*,*16*) ($n = 285$). Next, 50 men with biochemical recurrence after definitive treatment of prostate cancer who had no tumor lesions on ^{68}Ga-PSMA PET were randomly selected from the institution database (*17*) to serve as a control group. The flowchart of this study is displayed in Figure 1. Inclusion criteria were imaging with ^{68}Ga-PSMA PET/CT and data evaluable by the segmentation software. Patients who underwent ^{18}F-labeled PSMA PET/CT or PSMA-targeted PET/MRI were excluded.

Of 435 screened men with prostate cancer, 406 were eligible and were included in the study. Overall, 162 (40%) patients underwent the scan in a prospective setting (NCT02940262, NCT03042312, and ACTRN12615000912583), whereas 244 (60%) underwent the scan under compassionate-access programs. In a subanalysis, we identified 20 patients from the metastatic castration-resistant prostate cancer cohort who had a high disease burden on the baseline ^{68}Ga-PSMA PET at the initiation of ^{177}Lu-PSMA-RLT and received a follow-up scan after 2 treatment cycles, as previously described (Fig. 1) (*18*).

All scans were performed between October 2014 and August 2019. All patients gave written consent to undergo a clinical ^{68}Ga-PSMA PET scan. The need for study-specific consent was waived by the Ethics Committee.

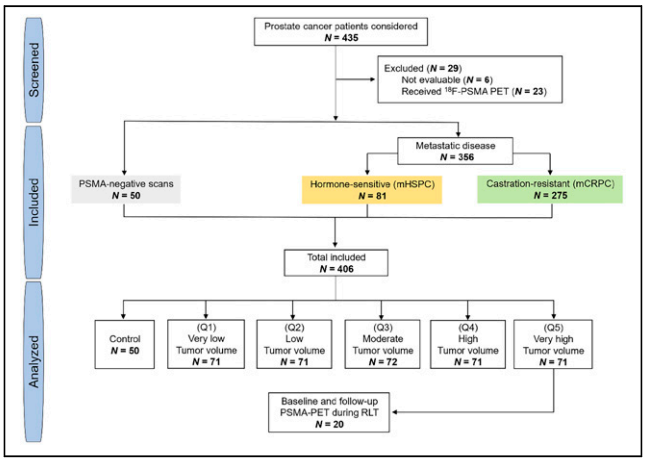

FIGURE 1. Study flowchart. mCRPC = metastatic castration-resistant prostate cancer; mHSPC = metastatic hormone-sensitive prostate cancer; Q = quintile.

Outcomes

The primary objective of this study was to determine the impact of total tumor burden on ^{68}Ga-PSMA uptake in normal organs on PET imaging. On the basis of reproducibility data that showed a normal variability of up to 30% between 2 SUV measurements of normal organs (*19*,*20*), the tumor sink effect was a priori defined as a 30% or greater decline in ^{68}Ga-PSMA uptake in normal organs, compared with the control group.

The secondary objective was to determine the impact of changes in tumor volume on normal-organ ^{68}Ga-PSMA uptake and the appearance of new lesions on the interim PET scan after 2 cycles of ^{177}Lu-PSMA-RLT. Patients were stratified into responders versus nonresponders to ^{177}Lu-PSMA-RLT on the basis of a PSMA tumor volume decline of 30% on the interim PET scan, as previously described (*18*).

Imaging Protocol

Patients received an average (±SD) of 155 ± 53 MBq of ^{68}Ga-PSMA-HBED-CC (PSMA-11) via complete intravenous injection. Image acquisition was started after an average of 64 ± 17 min after injection. Static, whole-body images were used (mid thighs to skull vertex). All scans were corrected for decay, scatter, and random coincidences. Data from the CT scan were used for attenuation correction. Images were acquired using GE Healthcare Discovery 710 ($n = 50$), Siemens Biograph mCT ($n = 244$), Siemens Biograph 64 ($n = 92$), and Siemens Biograph 16 ($n = 20$) scanners. All images were obtained in accordance with the ^{68}Ga-PSMA PET joint guideline of the European Association of Nuclear Medicine and the Society of Nuclear Medicine and Molecular Imaging, ensuring harmonized quantification (*21*). Standard vendor-provided image reconstructions were used. The applied reconstruction parameters are summarized in Supplemental Table 1 (supplemental materials are available at http://jnm.snmjournals.org).

Image Analyses

Tumor segmentation was performed centrally by a nuclear medicine physician using qPSMA software (*22*) to obtain total PSMA-positive tumor volume (PSMA-VOL). PSMA-VOL was categorized into 5 groups based on quintiles: very low (quintile 1: ≤20th percentile), low (quintile 2: 20th–40th percentiles), moderate (quintile 3: 40th–60th percentiles), high (quintile 4: 60th–80th percentiles), and very high (quintile 5: ≥80th percentile). Organs that typically exhibit moderate to high PSMA-ligand uptake were assessed: salivary glands, kidneys, liver, and spleen (*23*). The entire volume of each normal organ was segmented automatically using an in-house algorithm. The annotations obtained using the automatic algorithm were reviewed by a nuclear medicine physician using PET images and adjusted manually when necessary. SUV_{mean} and SUV_{max} not corrected for lean body mass or body surface area were obtained to measure ^{68}Ga-PSMA uptake in normal organs. The liver was not analyzed in patients with PSMA-positive liver metastases. Salivary glands not entirely included in the PET field of view were excluded from the analysis.

Statistical Analyses

Values were reported as mean ± SD or median and interquartile range (IQR). Correlations between PSMA-VOL and normal-organ tracer uptake were evaluated using the Spearman correlation coefficient (ρ) with a 2-tailed test for significance. Kruskal–Wallis testing was performed to compare the degree of ^{68}Ga-PSMA uptake in normal organs among the 6 tumor-burden groups (control, very low, low, moderate, high, and very high). Differences among groups were tested

for significance against no difference. A P value of 0.05 or less was considered statistically significant. The P values were not adjusted for multiple testing. Analyses were performed using SPSS Statistics, version 26.0 (IBM Corp.), and R Statistics (version 3.4.0).

RESULTS

Population characteristics are summarized in Table 1. Liver uptake was not analyzed in 40 patients because of PSMA-positive liver metastases. The salivary glands of 2 patients could not be delineated and were excluded from the analysis.

Tumor Volume and Organ SUV Measurements

The median SUV_{mean} of salivary glands, kidneys, liver, and spleen was 10.0 (IQR, 7.7–11.8), 26.0 (IQR, 20.0–33.4), 3.7 (IQR, 3.0–4.7), and 5.3 (IQR, 4.0–7.2), respectively (Fig. 2), whereas the median SUV_{max} was 21.3 (IQR, 16.9–27.0), 51.8 (IQR, 37.8–67.9), 9.7 (IQR, 7.8–11.8), and 10.1 (IQR, 8.0–12.8), respectively (Supplemental Fig. 1). The median PSMA-VOL was 302 cm^3 (IQR, 47–1,076 cm^3). The 20th, 40th, 60th, and 80th percentile of PSMA-VOL was 25, 189, 532, and 1,355 cm^3, respectively. The median PSMA-VOL in the very low ($n = 71$), low ($n = 71$), moderate ($n = 71$), high ($n = 72$), and very high ($n = 71$) groups was 5 cm^3 (IQR, 2–11 cm^3), 76 cm^3 (IQR, 46–123 cm^3), 302 cm^3 (IQR, 235–387 cm^3), 899 cm^3 (IQR, 685–1,078 cm^3), and 2,336 cm^3 (IQR, 1,852–3,080 cm^3), respectively. Examples of ^{68}Ga-PSMA PET studies for each tumor volume group are presented in Figure 3.

Correlations of Tumor Volume with Normal-Organ Uptake

PSMA-VOL showed a statistically significant moderate negative correlation with the SUV_{mean} of salivary glands ($r = -0.44$, $P < 0.001$), kidneys ($r = -0.34$, $P < 0.001$), and liver ($r = -0.30$, $P < 0.001$) and a statistically significant weak negative correlation with spleen SUV_{mean} ($r = -0.16$, $P = 0.002$). PSMA-VOL showed a statistically significant moderate negative correlation with the SUV_{max} of salivary glands ($r = -0.35$, $P < 0.001$) and a statistically significant weak negative correlation with kidneys ($r = -0.26$, $P < 0.001$), liver ($r = -0.23$, $P < 0.001$), and spleen SUV_{max} ($r = -0.19$, $P < 0.001$).

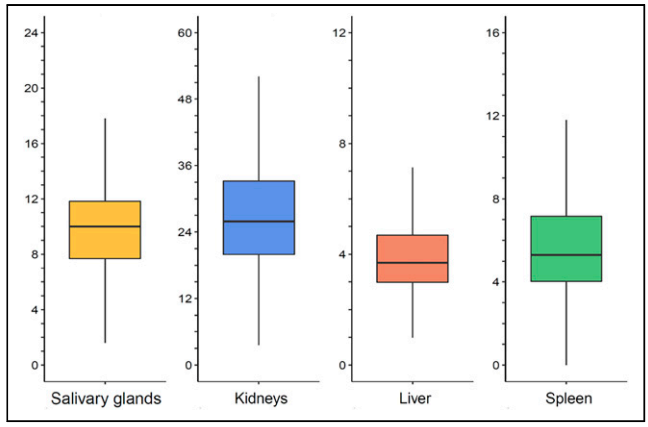

FIGURE 2. SUV_{mean} of normal organs. Horizontal lines represent median value.

Normal-Organ Uptake Stratified by Tumor Volume Groups

The absolute values and differences in SUVs of normal organs in the very low, low, moderate, high, and very high PSMA-VOL groups compared with the control group are given in Table 2, Figure 4, and Supplemental Figure 2. In general, a higher PSMA-VOL was associated with lower ^{68}Ga-PSMA uptake in normal organs.

The SUV_{mean} of salivary glands, kidneys, liver, and spleen was significantly lower in patients with a very high PSMA-VOL

TABLE 1
Characteristics of Patients

Characteristics	Control (n = 50)	mHSPC (n = 81)	mCRPC (n = 275)
Age (y)	71 (69–74)	69 (63–72)	72 (66–76)
Weight (kg)	86 (80–99)	81 (75–92)	80 (72–92)
Injected activity (MBq)	185 (183–196)	128 (96–153)	155 (112–195)
Acquisition time (min)	60 (55–66)	65 (59–82)	60 (53–67)
PSA (ng/mL)*	0.4 (0.2–0.8)	4.0 (1–11)	130 (37–431)
PSMA-VOL (cm^3)	0	7 (2–37)	563 (194–1,358)
Site of disease on PSMA-PET			
Bone	0	70 (86%)	256 (93%)
Lymph nodes	0	34 (42%)	202 (74%)
Bone + lymph nodes	0	27 (33%)	183 (67%)
Viscera†	0	10 (12%)	82 (30%)
Bone + lymph nodes + viscera	0	1 (1%)	59 (22%)

*Data missing for 10 patients.
†Viscera include lung, liver, rectum, pancreas, peritoneal, brain and adrenal.
mHSPC = metastatic hormone-sensitive prostate cancer; mCRPC = metastatic castration-resistant prostate cancer; PSA = prostate-specific antigen.
Qualitative data are number and percentage; continuous data are median and IQR.

RGB

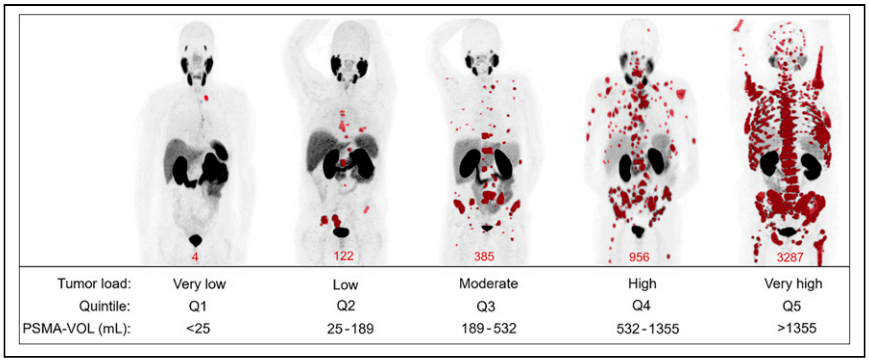

FIGURE 3. Examples of maximum-intensity-projection images of PSMA PET for each tumor load group. PSMA-positive tumor segmentation is highlighted in red.

than in the control group ($P < 0.001$), with an average difference of −38.1% (95% CI, −47.8%, −29.7%), −40.0% (95% CI, −50.3%, −31.1%), −43.2% (95% CI, −55.6%, −30.8%), and −34.9% (95% CI, −49.8%, −21.3%), respectively.

The SUV_{max} of salivary glands, kidneys, and liver was significantly lower in patients with a very high PSMA-VOL than in the control group ($P < 0.05$), with an average difference of −26.6% (95% CI, −38.9%, −15.1%), −28.4% (95% CI, −39.4%, −18.0%), and −17.9% (95% CI, −30.0%, −4.2%), respectively.

Changes in Tumor Volume and Normal Uptake

Of 20 patients included in this analysis, 10 (50%) were responders achieving a PSMA-VOL decline of at least 30% on the interim scan relative to baseline. The average change in PSMA-VOL in responders was −47.0% (95% CI, −55.7%, −38.4%), whereas in nonresponders it was +6.3% (95% CI, −14.4%, +26.9%). The average difference in SUV_{mean} of salivary glands, liver, kidneys and spleen in responders was +61.1% (95% CI, −3.5%, +125.7%; $P = 0.06$), +33.4% (95% CI, −17.2%, +83.9%; $P = 0.17$), +74.0% (95% CI, +8.7%, +139.2%; $P = 0.03$), and +61.8% (95% CI, +21.4%, +102.2%; $P = 0.007$), respectively. In nonresponders, the average change in salivary glands, kidneys, liver and spleen was −2.5% (95% CI, −15.3%, +10.3%; $P = 0.67$), +10.7% (95% CI, −6.1%, +28.3%; $P = 0.07$), +12.1% (95% CI, −6.1%, +30.3%; $P = 0.16$), and +23.8% (95% CI, −18.9%, +66.5%; $P = 0.24$), respectively. Individual changes in PSMA-VOL, SUV_{mean}, and SUV_{max} for normal organs in ^{68}Ga-PSMA PET are given in Supplemental Table 2. The appearance of new PSMA-positive lesions on interim scans was observed in 1 (10%) responder and 7 (70%) nonresponders.

DISCUSSION

In this multicenter retrospective analysis, patients with a high tumor burden demonstrated significantly lower normal-organ uptake on ^{68}Ga-PSMA PET. Our primary endpoint of an SUV difference numerically greater than 30% in salivary glands and kidneys compared with the control group was met in patients with a very high tumor volume (≥1,355 cm^3).

Controversial results on the tumor sink effect in PSMA-targeted PET have been reported. Gaertner et al. (*13*) found a decline of 36%–43%, 45%, 25%, and 19% of ^{68}Ga-PSMA uptake in salivary glands, kidneys, liver, and spleen, respectively, in metastatic castration-resistant prostate cancer patients who were classified visually as having a high PSMA-positive tumor burden on PET. In contrast, Werner et al. (*14*) found in ^{18}F-DCFPyL PET a significant correlation only for kidney uptake with PSMA-VOL. However, these results are not surprising, since only patients with early-stage prostate cancer having a low tumor burden were included (median PSA, 3.2 ng/mL) whereas a sink effect is expected to occur at high tumor volume levels. Limitations of these studies also include the small sample size, which was not powered for uptake correlation, use of a small region of interest for measuring tracer uptake in large organs (e.g., liver or spleen), and visual assessment of disease burden. To overcome these, in the present analysis we segmented semiautomatically on ^{68}Ga-PSMA PET the total disease burden and the entire volume of normal organs. Moreover, for a complete understanding of the associations between disease burden and normal uptake, we included patients from the entire spectrum of prostate cancer and categorized them into 6 subgroups: PSMA-negative, very low, low, moderate, high, and very high tumor volume.

The highest correlation of normal-organ uptake with tumor burden was noticed in salivary glands, followed by kidneys, liver, and, to a lower degree, spleen. However, the SUV_{mean} of kidneys and liver was significantly lower beginning with patients with a low tumor volume (25–189 cm^3), whereas for salivary glands it was significantly lower only in patients with high (532–1,355 cm^3) and very high (≥1,355 cm^3) tumor volumes. SUV_{mean} of normal organs had a weaker correlation with SUV. This observation underlines the importance of using SUV_{mean} over SUV_{max} for measuring tracer uptake in normal organs in PET imaging, which captures the entire organ uptake and does not limit the uptake to 1 voxel. Two limitations of SUV_{max} are worth mentioning here: the variability when structures with heterogeneous uptake are measured (e.g., liver) and the dependence on the reconstruction parameters (e.g., potential use of point-spread function). These limitations can have important implications, particularly in a multicentric setting in which the harmonization protocol can affect SUV_{max} findings.

Our study has clinical implications. When performing PSMA-targeted RLT, the therapeutic activity is limited because of potential toxicity to organs at risk. Salivary glands and kidneys are the main critical organs with the highest absorbed dose (*10*). Moreover, xerostomia was reported as the main reason for treatment discontinuation during ^{225}Ac-PSMA-RLT (*24*). Our findings suggest that candidates for ^{177}Lu-PSMA-RLT with a very high tumor volume (≥1,355 cm^3 for our analysis defined by quintiles) on the screening PSMA-PET have a significantly lower normal-organ uptake and might benefit from an increased therapeutic activity without exceeding the radiation dose limit for organs at risk.

A first attempt toward individualizing therapeutic activity for ^{177}Lu-PSMA-RLT was made by Hofman et al. (*5*), in a study in which ^{177}Lu-PSMA-617 activity was increased by up to 20% in heavily metastasized patients. Dosimetry data from the same cohort showed that a higher absorbed dose to tumor was associated with higher rates of PSA response and that tumor volume delineated on pretherapeutic ^{68}Ga-PSMA PET is inversely correlated with salivary gland and kidney absorbed radiation dose (*25*). Hence, the sink effect may represent a great opportunity for

TABLE 2
Comparison of PSMA-VOL Groups and ^{68}Ga-PSMA Uptake in Normal Organs

Organ	Tumor load group	PSMA-VOL (cm^3)	SUV_{mean}			SUV_{max}		
			Median	Difference from control (%)	*P*	Median	Difference from control (%)	*P*
Salivary gland	Control	0	11.0 (10.0–12.4)	—	—	21.8 (19.3–26.2)	—	—
	Very low	<25	10.3 (8.3–13.7)	−6.4 (−15.2, +3.4)	0.189	22.9 (18.3–29.5)	+5.0 (−4.0, +14.2)	0.585
	Low	25–189	11.0 (9.1–12.9)	+0.5 (−9.8, +10.5)	0.239	21.9 (18.1–29.2)	+0.5 (−9.1, +9.9)	0.768
	Moderate	189–532	10.8 (9.1–12.0)	−1.8 (−9.8, +5.1)	0.195	23.4 (20.1–29.0)	+7.3 (−2.5, +18.0)	0.352
	High	532–1,355	8.3 (6.6–10.3)	−24.5 (−33.3, −17.0)	<0.001	18.3 (13.8–22.5)	−16.0 (−7.2, −25.5)	<0.001
	Very high	>1,355	6.8 (5.5–9.4)	−38.1 (−47.8, −29.7)	<0.001	16.0 (11.2–23.0)	−26.6 (−15.1, −38.9)	<0.001
Kidney	Control	0	34.7 (26.4–37.8)	—	—	59.8 (49.5–68.1)	—	—
	Very low	<25	30.3 (23.0–35.8)	−12.6 (−22.0, +2.2)	0.125	55.4 (43.8–69.5)	−7.4 (−17.8, +3.1)	0.394
	Low	25–189	26.7 (20.0–33.9)	−23.0 (−34.1, −13.5)	0.001	52.6 (37.3–69.7)	−12.0 (−22.9, −1.4)	0.054
	Moderate	189–532	26.5 (19.3–32.8)	−23.6 (−32.0, −15.2)	<0.001	54.2 (37.4–71.2)	−9.4 (−12.5, +3.0)	0.085
	High	532–1,355	24.0 (18.9–31.4)	−30.8 (−42.1, −20.3)	<0.001	47.7 (35.2–65.3)	−20.2 (−30.5, −9.8)	0.005
	Very high	>1,355	20.8 (15.1–23.6)	−40.0 (−50.3, −31.1)	<0.001	42.8 (31.4–52.8)	−28.4 (−39.4, −18.0)	<0.001
Liver	Control	0	4.4 (3.6–5.5)	—	—	9.5 (8.2–11.2)	—	—
	Very low	<25	3.8 (3.2–5.2)	−13.6 (−25.0, +1.6)	0.070	11.0 (8.5–12.4)	15.8 (+2.4, +25.9)	0.073
	Low	25–189	3.9 (3.1–4.5)	−11.4 (−20.3, −3.0)	0.010	10.1 (7.5–11.6)	+6.3 (−4.1, +15.2)	0.886
	Moderate	189–532	3.9 (3.3–4.8)	−11.4 (−22.0, −1.7)	0.033	9.9 (8.5–12.2)	+4.2 (−9.8, +17.1)	0.451
	High	532–1,355	3.7 (3.0–4.9)	−15.9 (−25.9, −16.1)	0.008	9.3 (7.6–11.6)	−2.1 (−11.8, +7.9)	0.842
	Very high	>1,355	2.5 (1.8–3.5)	−43.2 (−55.6, −30.8)	<0.001	7.8 (6.4–10.6)	−17.9 (−30.0, −4.2)	0.017
Spleen	Control	0	6.3 (4.6–8.2)	—	—	10.3 (8.2–13.4)	—	—
	Very low	<25	5.5 (4.2–6.8)	−12.7 (−25.5, +1.2)	0.074	10.9 (9.3–12.6)	+5.8 (−6.1, +17.6)	0.384
	Low	25–189	5.3 (4.5–7.6)	−14.9 (−30.0, +2.4)	0.175	10.2 (8.2–13.7)	−1.0 (−9.8, +8.0)	0.888
	Moderate	189–532	5.9 (4.4–7.8)	−6.3 (−18.9, +6.2)	0.422	11.0 (8.4–13.9)	+6.8 (−6.2, +19.3)	0.492
	High	532–1,355	4.8 (3.9–7.2)	−23.8 (−37.3, −6.8)	0.012	9.2 (7.5–12.9)	−10.7 (−23.9, +3.4)	0.271
	Very high	>1,355	4.1 (3.3–6.0)	−34.9 (−49.8, −21.3)	<0.001	9.1 (6.4–12.2)	−11.7 (−24.4, +1.9)	0.068

Data are median and IQR, or difference and 95% CI.

RGB

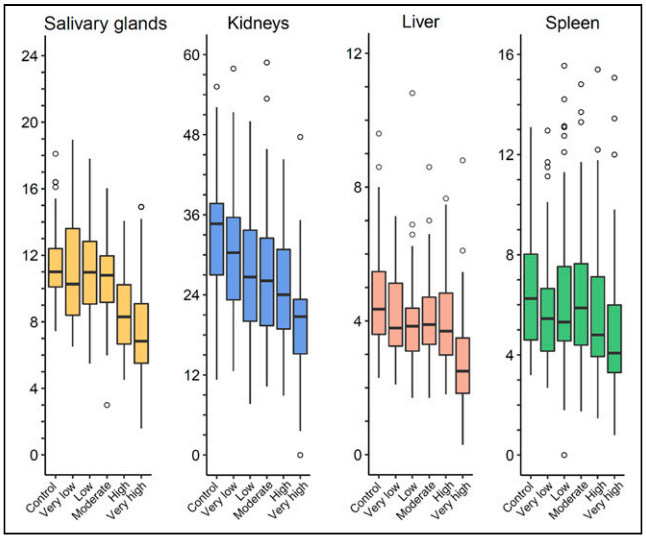

FIGURE 4. SUV_{mean} of normal organs stratified by tumor load.

^{177}Lu-PSMA-RLT to safely increase therapeutic activity in order to improve antitumor efficacy. Besides toxicity, it might also be logical to administer a higher treatment activity when the tumor load is higher, in order to avoid undertreatment.

Overall, the present study establishes tumor sequestration as a major factor affecting ^{68}Ga-PSMA biodistribution in patients with a high disease burden, which leads to a sink effect that decreases activity concentrations in normal organs. In addition, we found that changes in tumor volume during ^{177}Lu-PSMA-RLT impact the normal uptake on follow-up ^{68}Ga-PSMA PET images. This finding emphasizes the potential utility of repeated dosimetry studies during ^{177}Lu-PSMA-RLT when individualizing therapeutic dosage. Only 1 patient (without a decrease in ^{68}Ga-PSMA uptake in normal organs; Supplemental Table 2) had new lesions on the follow-up scan, suggesting that new lesions on PSMA posttreatment scans are likely to be treatment-related. Nevertheless, additional studies investigating the impact of the sink effect on intratumor heterogeneity are warranted to provide additional insights on this phenomenon.

Strengths of this study include the multicenter setting, large patient population, and use of full quantitative measurements for tumor burden assessment. The major limitation of this study is the use of a single static PET image protocol, and thus, our results should be interpreted with caution in the framework of ^{177}Lu-PSMA-RLT. In addition, we are unable to analyze the influence of potential effects arising from different specific activities. However, given the low half-life of ^{68}Ga and a standardized production, no large-scale ($>10^2$) difference might be present. Further, we used only SUV normalized to body weight as a quantitative parameter of PET signal. Alternative quantitative parameters have been described in the literature, that is, SUV normalized to lean body mass (*26*) or the ratio of tumor uptake to blood-pool uptake (*27*), although only at a research level. Further studies to support their implementation in clinical practice are awaited. Correlations with dosimetry data with multiple time points are warranted to establish pretherapeutic PSMA-targeted PET as a quantitative tool for individualizing therapeutic doses.

CONCLUSION

Tumor sequestration affects ^{68}Ga-PSMA biodistribution by decreasing the activity concentration in normal organs, confirming the tumor sink effect. A relevant sink effect was noticed in patients with a very high tumor burden ($\geq$1,355 cm^3). Because of favorable uptake ratios, PSMA-targeted RLT with increased activity regimens should be assessed in patients with a very high tumor volume. Repeated dosimetry during PSMA-targeted RLT should be considered, in order not to miss the impact of changes in tumor burden on dose distribution. Further studies are warranted to establish pretherapeutic PSMA-targeted PET as a tool for individual activity adaptation in PSMA-targeted RLT.

DISCLOSURE

This work was partially supported by the Jonsson Comprehensive Cancer Center fellowship award. Andrei Gafita is the recipient of the Jonsson Comprehensive Cancer Center fellowship award and the Dr. Christiaan Schiepers postdoctoral fellowship award. Jeremie Calais is supported by the Prostate Cancer Foundation (2020 Young Investigator Award 20YOUN05, 2019 Challenge Award 19CHAL02) and the Society of Nuclear Medicine and Molecular Imaging (2019 Molecular Imaging Research Grant for Junior Academic Faculty) and reports prior consulting activities outside the submitted work for Advanced Accelerator Applications, Blue Earth Diagnostics, Curium Pharma, GE Healthcare, Janssen Pharmaceuticals, Progenics Pharmaceuticals, Radiomedix, and Telix Pharmaceuticals. Michael Hofman is supported by grants from the Prostate Cancer Foundation, Movember Foundation, Australian Government Medical Research Future Fund, Prostate Cancer Foundation of Australia, and U.S. Department of Defence and reports honoraria for lectures from Astellas, Janssen, Mundipharma and advisory fees from Merck/MSD. Wolfgang Fendler received financial support from the German Research Foundation (Deutsche Forschungsgemeinschaft grant FE1573/3-1/659216), Mercator Research Center Ruhr (MERCUR, An-2019-0001), IFORES (D/107-81260, D/107-30240), Doktor Robert Pfleger-Stiftung, and Wiedenfeld-Stiftung/Stiftung Krebsforschung Duisburg; was a consultant for Endocyte and BTG; and received fees from RadioMedix and Bayer outside the submitted work. Hui Wang received financial support from the China Scholarship Council. Fernando Navarro received financial support from the German Research Foundation (Deutsche Forschungsgemeinschaft research training group grant GRK 2274). Matthias Eiber reports prior consulting activities for Blue Earth Diagnostics, Progenics Pharmaceuticals, and Point Biopharma and a patent application for rhPSMA outside the submitted work. Johannes Czernin is a founder and board member of, and holds equity in, Sofie Biosciences and Trethera Therapeutics and was a consultant for Endocyte Inc. (VISION trial steering committee), Actinium Pharmaceuticals, and Point Biopharma outside the submitted work. Intellectual property is patented by the University of California and licensed to Sofie Biosciences and Trethera Therapeutics. Ken Herrmann reports personal fees from Bayer, Sofie Biosciences, SIRTEX, Adacap, Curium, Endocyte, BTG, IPSEN, Siemens Healthineers, GE Healthcare, Amgen, Novartis, ymabs, Bain Capital, and MPM Capital outside the submitted work; other fees from Sofie Biosciences; nonfinancial support from ABX; and grants from BTG. No other potential conflict of interest relevant to this article was reported.

KEY POINTS

QUESTION: Does the tumor burden impact the biodistribution of ^{68}Ga-PSMA PET?

PERTINENT FINDINGS: In this international multicenter, retrospective study, we observed a significant negative correlation between PSMA-positive tumor burden and ^{68}Ga-PSMA PET uptake in normal organs—that is, salivary glands, kidneys, liver, and spleen. Patients with a very high tumor burden (≥1,355 cm^3 for our analysis defined by quintiles) had a significantly lower uptake of ^{68}Ga-PSMA in normal organs.

IMPLICATIONS FOR PATIENT CARE: Our findings suggest that candidates for ^{177}Lu-PSMA-RLT with a very high tumor volume on screening PSMA-PET have significantly lower normal-organ uptake and might benefit from an increased therapeutic activity without exceeding the radiation dose limit for organs at risk.

REFERENCES

1. Pfob CH, Ziegler S, Graner FP, et al. Biodistribution and radiation dosimetry of ^{68}Ga-PSMA HBED CC: a PSMA specific probe for PET imaging of prostate cancer. *Eur J Nucl Med Mol Imaging.* 2016;43:1962–1970.
2. Beauregard JM, Hofman MS, Kong G, Hicks RJ. The tumour sink effect on the biodistribution of ^{68}Ga-DOTA-octreotate: implications for peptide receptor radionuclide therapy. *Eur J Nucl Med Mol Imaging.* 2012;39:50–56.
3. Viglianti BL, Wale DJ, Wong KK, et al. Effects of tumor burden on reference tissue standardized uptake for PET imaging: modification of PERCIST criteria. *Radiology.* 2018;287:993–1002.
4. Love C, Din AS, Tomas MB, Kalapparambath TP, Palestro CJ. Radionuclide bone imaging: an illustrative review. *Radiographics.* 2003;23:341–358.
5. Hofman MS, Violet J, Hicks RJ, et al. [^{177}Lu]-PSMA-617 radionuclide treatment in patients with metastatic castration-resistant prostate cancer (LuPSMA trial): a single-centre, single-arm, phase 2 study. *Lancet Oncol.* 2018;19:825–833.
6. Emmett L, Crumbaker M, Ho B, et al. Results of a prospective phase 2 pilot trial of ^{177}Lu-PSMA-617 therapy for metastatic castration-resistant prostate cancer including imaging predictors of treatment response and patterns of progression. *Clin Genitourin Cancer.* 2019;17:15–22.
7. Violet J, Sandhu S, Iravani A, et al. Long-term follow-up and outcomes of retreatment in an expanded 50-patient single-center phase II prospective trial of ^{177}Lu-PSMA-617 theranostics in metastatic castration-resistant prostate cancer. *J Nucl Med.* 2020;61:857–865.
8. Privé BM, Janssen MJR, van Oort IM, et al. Lutetium-177-PSMA-I&T as metastases directed therapy in oligometastatic hormone sensitive prostate cancer, a randomized controlled trial. *BMC Cancer.* 2020;20:884.
9. Hofman MS, Hicks RJ. Peptide receptor radionuclide therapy for neuroendocrine tumours: standardized and randomized, or personalized? *Eur J Nucl Med Mol Imaging.* 2014;41:211–213.
10. Okamoto S, Thieme A, Allmann J, et al. Radiation dosimetry for ^{177}Lu-PSMA I&T in metastatic castration-resistant prostate cancer: absorbed dose in normal organs and tumor lesions. *J Nucl Med.* 2017;58:445–450.
11. Hofman MS, Lawrentschuk N, Francis RJ, et al. Prostate-specific membrane antigen PET-CT in patients with high-risk prostate cancer before curative-intent surgery or radiotherapy (proPSMA): a prospective, randomised, multicentre study. *Lancet.* 2020;395:1208–1216.
12. Wang J, Zang J, Wang H, et al. Pretherapeutic ^{68}Ga-PSMA-617 PET may indicate the dosimetry of ^{177}Lu-PSMA-617 and ^{177}Lu-EB-PSMA-617 in main organs and tumor lesions. *Clin Nucl Med.* 2019;44:431–438.
13. Gaertner FC, Halabi K, Ahmadzadehfar H, et al. Uptake of PSMA-ligands in normal tissues is dependent on tumor load in patients with prostate cancer. *Oncotarget.* 2017;8:55094–55103.
14. Werner RA, Bundschuh RA, Bundschuh L, et al. Semiquantitative parameters in PSMA-targeted PET imaging with [^{18}F]DCFPyL: impact of tumor burden on normal organ uptake. *Mol Imaging Biol.* 2020;22:190–197.
15. Gafita A, Fendler WP, Hui W, et al. Efficacy and safety of ^{177}Lu-labeled prostate-specific membrane antigen radionuclide treatment in patients with diffuse bone marrow involvement: a multicenter retrospective study. *Eur Urol.* 2020;78:148–154.
16. Gafita A, Calais J, Grogan TR, et al. Nomograms to predict outcome after LuPSMA radionuclide therapy in men with metastatic castration resistant prostate cancer: an international multicenter retrospective study. *Lancet Oncol.* 2021;22:1115–1125.
17. Fendler WP, Calais J, Eiber M, et al. Assessment of ^{68}Ga-PSMA-11 PET accuracy in localizing recurrent prostate cancer: a prospective single-arm clinical trial. *JAMA Oncol.* 2019;5:856–863.
18. Gafita A, Weber W, Tauber R, Eiber M. Predictive value of interim PSMA PET during ^{177}Lu-PSMA radioligand therapy for overall survival in patients with advanced prostate cancer [abstract]. *J Nucl Med.* 2019;60(suppl 1):73.
19. Pollard JH, Raman C, Zakharia Y, et al. Quantitative test-retest measurement of ^{68}Ga-PSMA-HBED-CC in tumor and normal tissue. *J Nucl Med.* 2020;61:1145–1152.
20. olde Heuvel J, de Wit-van der Veen BJ, Donswijk ML, Slump CH, Stokkel MPM. Day-to-day variability of [^{68}Ga]Ga-PSMA-11 accumulation in primary prostate cancer: effects on tracer uptake and visual interpretation. *EJNMMI Res.* 2020;10:132.
21. Fendler WP, Eiber M, Beheshti M, et al. ^{68}Ga-PSMA PET/CT: joint EANM and SNMMI procedure guideline for prostate cancer imaging—version 1.0. *Eur J Nucl Med Mol Imaging.* 2017;44:1014–1024.
22. Gafita A, Bieth M, Krönke M, et al. qPSMA: semiautomatic software for whole-body tumor burden assessment in prostate cancer using ^{68}Ga-PSMA11 PET/CT. *J Nucl Med.* 2019;60:1277–1283.
23. Pfob CH, Ziegler S, Graner FP, et al. Biodistribution and radiation dosimetry of ^{68}Ga-PSMA HBED CC: a PSMA specific probe for PET imaging of prostate cancer. *Eur J Nucl Med Mol Imaging.* 2016;43:1962–1970.
24. Feuerecker B, Tauber R, Knorr K, et al. Activity and adverse events of actinium-225-PSMA-617 in advanced metastatic castration-resistant prostate cancer after failure of lutetium-177-PSMA. *Eur Urol.* 2021;79:343–350.
25. Violet J, Jackson P, Ferdinandus J, et al. Dosimetry of ^{177}Lu-PSMA-617 in metastatic castration-resistant prostate cancer: correlations between pretherapeutic imaging and whole-body tumor dosimetry with treatment outcomes. *J Nucl Med.* 2019;60:517–523.
26. Gafita A, Calais J, Franz C, et al. Evaluation of SUV normalized by lean body mass (SUL) in ^{68}Ga-PSMA11 PET/CT: a bi-centric analysis. *EJNMMI Res.* 2019;9:103.
27. Jansen BHE, Kramer GM, Cysouw MCF, et al. Healthy tissue uptake of ^{68}Ga-prostate specific membrane antigen (PSMA), ^{18}F-DCFPyL, ^{18}F-fluoromethylcholine (FCH) and ^{18}F-dihydrotestosterone (FDHT). *J Nucl Med.* 2019;60:1111–1117.